EPJ Web of Conferences **216**, 04006 (2019) https://doi.org/10.1051/epjconf/201921604006
ARENA 2018

Updated Calibration of the LOFAR Low-Band Antennas

K. Mulrey[1,⋆], *A.* Bonardi[2], *S.* Buitink[1], *A.* Corstanje[2], *H.* Falcke[2,3,4], *B.M.* Hare[5], *J.* Hörandel[1,2,3], *P.* Mitra[1], *A.* Nelles[9,10], *J.P.* Rachen[2], *L.* Rossetto[2], *P.* Schellart[2,6], *O.* Scholten[5,7], *S.* ter Veen[2,4], *S.* Thoudam[2,8], *T.N.G.* Trinh[5], and *T.* Winchen[1]

[1] *Astrophysical Institute, Vrije Universiteit Brussel, Pleinlaan 2, 1050 Brussels, Belgium*
[2] *Department of Astrophysics/IMAPP, Radboud University, P.O. Box 9010, 6500 GL Nijmegen, The Netherlands*
[3] *NIKHEF, Science Park Amsterdam, 1098 XG Amsterdam, The Netherlands*
[4] *Netherlands Institute of Radio Astronomy (ASTRON), Postbus 2, 7990 AA Dwingeloo, The Netherlands*
[5] *KVI-CART, University Groningen, P.O. Box 72, 9700 AB Groningen*
[6] *Department of Astrophysical Sciences, Princeton University, Princeton, NJ 08544, USA*
[7] *Interuniversity Institute for High-Energy, Vrije Universiteit Brussel, Pleinlaan 2, 1050 Brussels, Belgium*
[8] *Department of Physics and Electrical Engineering, Linnéuniversitetet, 35195 Växjö, Sweden*
[9] *DESY, Platanenallee 6, 15738 Zeuthen, Germany*
[10] *Humboldt-Universität zu Berlin, Institut für Physik, Newtonstr. 15, 12489 Berlin, Germany*

Abstract. The LOw-Frequency ARray (LOFAR) telescope measures radio emission from air showers. In order to interpret the data, an absolute, frequency dependent calibration is required. Due to a growing need for a better understanding of the measured frequency spectrum, we revisit the calibration of the LOFAR antennas in the range of 30–80 MHz. Using the galactic radio emission and a detailed model of the LOFAR signal chain, we find a calibration that provides an absolute energy scale and allows us to study frequency dependent features in measured air shower signals.

1 Introduction

Using radio measurements, air shower features such as the energy and atmospheric depth of the shower maximum can be reconstructed. The LOw-Frequency ARray (LOFAR) telescope is particularly well suited to measuring air showers because of its dense antenna spacing [1, 2]. Shower properties such as X_{max}, wavefront shape, and circular polarization have been measured [3–5]. Ongoing efforts to understand the shape of the power spectra of radio emission are underway [6]. Critical to all these studies is a calibration of the LOFAR system response. A calibration is required to reconstruct the physical voltage at the load of the antenna from the signal recorded in units of ADC counts, providing an absolute conversion factor for the signal and correcting for frequency dependent gains and losses in the system.

Previously, two techniques have been used to calibrate the LOFAR low-band antennas (LBAs) which operate in the 30–80 MHz band [7]. The first used an externally calibrated reference antenna. This method suffers from the difficulties of calibrating antennas at low frequencies. The reference

⋆e-mail: kmulrey@vub.be, funded by ERC No 640130

antenna has been calibrated in two independent ways, yielding different spectral responses. These differences propagate into the LOFAR calibration. The second method used the galactic emission as a calibration source. This method requires knowing the contributions of electronic noise to the system, and the original galactic calibration is limited by the systematic uncertainty of the electronic noise. In this contribution we revisit the galactic method, characterizing electronic noise in detail so as to provide an absolute, frequency dependent calibration function.

2 Calibration method

Galactic emission in combination with electronic noise in the signal chain makes up the majority of background in LOFAR data. By modeling the expected background and comparing it to the measured background, we can determine the proper calibration function. The expected galactic temperature is derived using LFmap simulation software [8], and converted into a voltage in the LBAs using a simulated antenna model, as described in [7]. From there, the signal propagates through the signal chain where it is amplified and digitized. Figure 1 shows a schematic of the signal chain, following galactic power, P_{sky}, to measured power, P_M. There are gains in the active antenna amplifier, $G_{ant}(\nu)$,

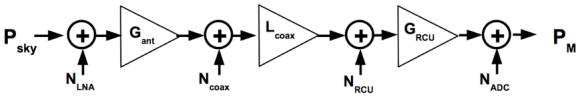

Figure 1. LOFAR signal chain, following sky power, P_{sky} to recorded power, P_M. Gains, losses, and electronic noise additions are shown.

losses in coaxial cables, $L_{coax}(\nu)$, and gains in the receiving unit, $G_{RCU}(\nu)$, where the signal is amplified and digitized. At each stage, noise is introduced, signified by the values N_{LNA}, N_{coax}, N_{RCU}, and N_{ADC}. The noise values are not known beforehand, and are determined using a fitting procedure which makes use of the time variation of the galactic signal. The difference between simulated power and measured power over 24 hours is minimized in 1 MHz bins. With the noise values found, the calibration function is comprised of each frequency dependent gain and loss in the system, as well as an overall scale factor.

3 Results

The calibration function based on the new method is shown in Figure 2, with the narrow band representing statistical uncertainties and the wide band showing systematic uncertainties, which total 14% below 77 MHz. The statistical uncertainties are due to event-to-event fluctuations. The systematic uncertainties are due to the uncertainty in the galaxy model and electronic noise, with uncertainties from the galaxy model dominating. The calibrations derived using an external reference antenna are also shown, with different lines resulting from the conflicting calibrations of the source antenna itself.

We compare the calibrated frequency spectra of measured cosmic ray signals with CoREAS simulations [9]. We look at the 20 strongest LOFAR events, and compare the log fit of the power spectra to simulations, comparing the magnitude of the slope, and the consistency of the slope over the 30–80 MHz band. More than 2500 individual signals are used for the study. For each signal, LOFAR data are calibrated with the new galaxy method and each of the calibrations resulting from the reference antenna method. In this frequency range, the shape of the power spectrum is expected to be exponential. A log fit is done for each spectrum in the ranges 30–58 MHz and 62–78 MHz, excluding the

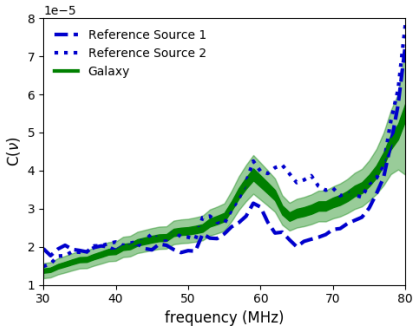

Figure 2. Calibration function for LOFAR data as determined using galactic emission and electronic noise (in green), and compared to the calibration functions derived using a reference source (blue) The different reference source calibrations come from different calibrations of the reference source itself. The width of the dark green line represents statistical uncertainties. The frequency dependent systematic uncertainties are indicated by the light green band, and reach a maximum of 14 % below 77 MHz.

LBA resonance frequency. Histograms of the differences in slope in each band for each data set are shown in Figure 3. The reference antenna calibrations show clear offsets in the different bands. There is promising agreement between the data calibrated with the new galaxy method and simulations.

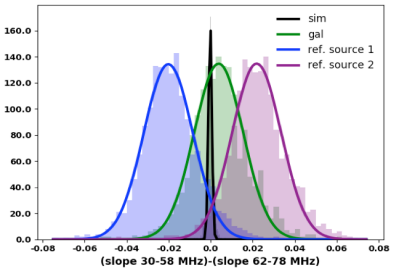

Figure 3. Histogram showing the difference between the slopes before (30–58 MHz) and after (62–78 MHz) the LBA resonance frequency, for ~ 2500 signals. CoREAS simulations are shown, as well as log slopes for measured power spectra calibrated with the new galaxy method, and the calibrations resulting from different characterizations of the reference antenna.

4 Conclusion

We revisited the calibration of the LOFAR LBAs using galactic emission, modeling each step in the signal chain in order to understand the electronic noise introduced into the system. Using this method, we arrived at a new absolute and frequency dependent calibration with a maximum of 14% systematic uncertainty below 77 MHz. A comparison of the log fit slopes of calibrated, measured power spectra and simulated power spectra shows promising agreement.

References

[1] M.P. van Haarlem et al., Astronomy and Astrophysics **556**, 56 (2013)
[2] P. Schellart et al., Astronomy and Astrophysics **560** (2013)
[3] S. Buitink et al., Nature **531**, 70 (2016)
[4] A. Corstanje et al., Astropart. Phys. **61**, 22 (2015), 1404.3907
[5] O. Scholten et al., Phys. Rev. **D94**, 103010 (2016), 1611.00758
[6] L. Rossetto et al., Proceedings of the 35th ICRC, Busan, South Korea **PoS(ICRC2017)329** (2017)
[7] A. Nelles et al., JINST **10**, P11005 (2015), 1507.08932
[8] E. Polisensky, *Lfmap: A low frequency sky map generating program* (2007), http://www.faculty.ece.vt.edu/swe/lwa/memo/lwa0111.pdf
[9] T. Huege, M. Ludwig, C.W. James, AIP Conf. Proc. **1535**, 128 (2013), 1301.2132